

# Anti-flow of $K_s^0$ Mesons in 6 AGeV Au + Au Collisions

P. Chung<sup>(1)</sup>, N. N. Ajitanand<sup>(1)</sup>, J. M. Alexander<sup>(1)</sup>, M. Anderson<sup>(5)</sup>, D. Best<sup>(3)</sup>, F.P. Brady<sup>(5)</sup>, T. Case<sup>(3)</sup>, W. Caskey<sup>(5)</sup>, D. Cebra<sup>(5)</sup>, J.L. Chance<sup>(5)</sup>, B. Cole<sup>(10)</sup>, K. Crowe<sup>(3)</sup>, A. Das<sup>(2)</sup>, J.E. Draper<sup>(5)</sup>, M.L. Gilkes<sup>(1)</sup>, S. Gushue<sup>(1,8)</sup>, M. Heffner<sup>(5)</sup>, A.S. Hirsch<sup>(6)</sup>, E.L. Hjort<sup>(6)</sup>, L. Huo<sup>(12)</sup>, M. Justice<sup>(4)</sup>, M. Kaplan<sup>(7)</sup>, D. Keane<sup>(4)</sup>, J.C. Kintner<sup>(11)</sup>, J. Klay<sup>(5)</sup>, D. Krofcheck<sup>(9)</sup>, R. A. Lacey<sup>(1)</sup>, J. Lauret<sup>(1)</sup>, M.A. Lisa<sup>(2)</sup>, H. Liu<sup>(4)</sup>, Y.M. Liu<sup>(12)</sup>, R. McGrath<sup>(1)</sup>, Z. Milosevich<sup>(7)</sup>, G. Odyniec<sup>(3)</sup>, D.L. Olson<sup>(3)</sup>, S. Y. Panitkin<sup>(4)</sup>, C. Pinkenburg<sup>(1)</sup>, N.T. Porile<sup>(6)</sup>, G. Rai<sup>(3)</sup>, H.G. Ritter<sup>(3)</sup>, J.L. Romero<sup>(5)</sup>, R. Scharenberg<sup>(6)</sup>, L. Schroeder<sup>(3)</sup>, B. Srivastava<sup>(6)</sup>, N.T.B Stone<sup>(3)</sup>, T.J.M. Symons<sup>(3)</sup>, T. Wienold<sup>(3)</sup>, R. Witt<sup>(4)</sup>, J. Whitfield<sup>(7)</sup>, L. Wood<sup>(5)</sup>, and W.N. Zhang<sup>(12)</sup>  
(E895 Collaboration)

<sup>(1)</sup>*Depts. of Chemistry and Physics, SUNY Stony Brook, New York 11794-3400*

<sup>(2)</sup>*Ohio State University, Columbus, Ohio 43210*

<sup>(3)</sup>*Lawrence Berkeley National Laboratory, Berkeley, California, 94720*

<sup>(4)</sup>*Kent State University, Kent, Ohio 44242*

<sup>(5)</sup>*University of California, Davis, California, 95616*

<sup>(6)</sup>*Purdue University, West Lafayette, Indiana, 47907-1396*

<sup>(7)</sup>*Carnegie Mellon University, Pittsburgh, Pennsylvania 15213*

<sup>(8)</sup>*Brookhaven National Laboratory, Upton, New York 11973*

<sup>(9)</sup>*University of Auckland, Auckland, New Zealand*

<sup>(10)</sup>*Columbia University, New York, New York 10027*

<sup>(11)</sup>*St. Mary's College, Moraga, California 94575*

<sup>(12)</sup>*Harbin Institute of Technology, Harbin, 150001 P. R. China*

We have measured the sideward flow of neutral strange ( $K_s^0$ ) mesons in 6 AGeV Au + Au collisions. A prominent anti-flow signal is observed for an impact parameter range ( $b \lesssim 7$  fm) which spans central and mid-central events. Since the  $K_s^0$  scattering cross section is relatively small in nuclear matter, this observation suggests that the in-medium kaon vector potential plays an important role in high density nuclear matter.

PACS 25.70.+r, 25.70.Pq

The production and properties of strange particles can provide an important probe of hot and dense nuclear matter [1,2]. They can give insight into the fundamental aspects of chiral symmetry restoration at high baryon density and/or temperature as well as information relevant to neutron stars [3–6]. Recent theories of kaon propagation in nuclei all predict an important role for the in-medium kaon-nucleon potential [7–11]. This potential is comprised of two parts: (1) an attractive s-wave scalar interaction, which can be linked to chiral symmetry breaking via the mass of the strange quark, and (2) a vector potential which is thought to be repulsive for kaons but attractive for anti-kaons.

The repulsive kaon-nucleon interaction can lead to a net repulsion of kaons away from nucleons resulting in the anti-flow of the kaons [12]. In fact, it has been argued that the sideward and elliptic flow pattern of kaons in relativistic heavy ion reactions, can provide a good probe for the influence of both the vector and scalar components of the kaon potential [12,13]. A recent measurement has indicated essentially zero sideward flow for the  $K^+$ s and  $K_s^0$ 's produced in 1.93 AGeV  $^{58}\text{Ni} + ^{58}\text{Ni}$  collisions. This

result has been attributed to the repulsive nature of the kaon-nucleon potential [14]. However, an alternative interpretation involving rescattering effects has been shown to account for the data [15]. The observation of an out-of-plane or negative elliptic flow of  $K^+$  mesons in 1 AGeV Au + Au collisions has been associated with the repulsive part of the  $K^+N$  potential [16]. Nonetheless, a general consensus on the nature of the kaon-nucleon potential has not been reached.

Flow measurements for  $K_s^0$  mesons can serve as a unique probe of the kaon-nucleon potential in that they avoid possible complications which could result from the Coulomb interaction between a charged kaon and the associated emitting system. Such measurements have been sparse because the relatively short life-time  $\tau$ , of the  $K_s^0$  ( $c\tau=2.68$  cm) imposes the requirement of a large acceptance device with high detection efficiency and very good momentum resolution. In this letter we report on the use of such a device – the E895 Time Projection Chamber (TPC) [17] – to make detailed measurements of the flow of neutral strange  $K_s^0$  mesons in 6 AGeV Au + Au collisions. The data from these measurements show prominent signatures for the anti-flow of  $K_s^0$  for both central and mid-central collisions, suggesting significant in-medium effects for these particles. The kaon potential, rather than that of the antikaon, is expected to dominate in the present study, since Relativistic Quantum Molecular Dynamics (RQMD) [18] calculations suggest an antikaon  $\bar{K}^0$  contribution of  $\lesssim 10\%$  in our data sample. Preliminary results from this work have been reported [19].

The measurements have been performed with the E895 detector system at the Alternating Gradient Synchrotron at the Brookhaven National Laboratory. This system in-

cludes a TPC [17] and a multi-sampling ionization chamber (MUSIC) [20]. Details on the detector system have been reported earlier [21,22]. The data presented here reflect the excellent coverage, continuous 3D-tracking, and particle identification capabilities of the TPC. All are important for the efficient detection and reconstruction of the neutral strange  $K_s^0$  mesons.

The  $K_s^0$ 's have been reconstructed from their pion decay-daughters  $K_s^0 \rightarrow \pi^+ + \pi^-$  (branching ratio  $\sim 69\%$ ) using the following procedure. First, all TPC tracks in an event were reconstructed along with the calculation of an overall event vertex. Second, each  $\pi^+ \pi^-$  pair was considered and their point of closest approach calculated.  $\pi^+ \pi^-$  pairs whose trajectories intersected at a point other than the main vertex were then evaluated to yield invariant mass  $m_{inv}$  and momentum. All of these hypothesized  $K_s^0$ 's with  $0.4 < m_{inv} < 0.6$  GeV/ $c^2$  were then passed through a fully connected feedforward multilayered neural network [23] trained to separate "true"  $K_s^0$ 's from the combinatoric background. The network was trained from a set consisting of "true"  $K_s^0$ 's and a set consisting of combinatoric background respectively. "True"  $K_s^0$ 's were generated by tagging and embedding simulated  $K_s^0$ 's in raw data events in a detailed GEANT simulation of the TPC. The background or "fake"  $K_s^0$ 's were generated via mixed events in which the candidate daughter particles of the  $K_s^0$  ( $\pi^+ \pi^-$ ) were chosen from different data events.

The resulting experimental invariant mass distribution for  $K_s^0$ 's is shown in Fig. 1. The distribution has been obtained for central and mid-central events (charged particle multiplicity  $\geq 100$ ) in which one or more  $K_s^0$ 's have been detected. This multiplicity distribution is estimated to correspond to an impact-parameter range,  $b \lesssim 7$  fm. The distribution shown in Fig. 1 is clearly peaked at the invariant mass expected for the  $K_s^0$  ( $\sim .5$  GeV), and the excellent peak to background ratio clearly demonstrates the reliability with which the neural network is able to separate real  $K_s^0$ 's from the combinatoric background. Fig. 2a, shows the uncorrected (for detection efficiency) decay-length distribution in the rest frame of the  $K_s^0$ 's, i.e.,  $d_i / \gamma_i \beta_i$ , where  $d_i$  is the laboratory distance from the main vertex to the decay vertex of each  $K_s^0$ ,  $i$ . The distribution is shown for the same  $K_s^0$ 's used to construct the invariant mass distribution shown in Fig. 1. The distribution is characterized by a prominent exponential tail. The apparent deficit below  $ct \sim 4$  cm reflects the difficulty of  $K_s^0$  reconstruction in the region of high track density near to the main event vertex. An exponential fit to the data over a region for which the detection efficiency was determined to be constant (7 - 11 cm), yields a  $c\tau$  value of  $2.74 \pm 0.07$  cm. This value is close to the expected value of 2.68 cm and therefore serves as further confirmation that the neural network does indeed separate true  $K_s^0$ 's from the combinatoric background. The reconstruction procedure produces a raw yield of  $\sim .03$   $K_s^0$ 's per event.

It is important to establish that the procedure used to train the neural network does not lead to the spurious

"creation" of  $K_s^0$ 's. To do this, we have processed "fake"  $K_s^0$ 's through the neural network. Fig. 2b shows input (dashed histogram) and output (solid histogram) invariant mass distributions for "fake"  $K_s^0$ 's generated via the mixed event procedure discussed above. The absence of a peak (at the  $K_s^0$  mass) in the output distribution demonstrates that the neural network is properly trained and does not "create" spurious  $K_s^0$ 's.

Our flow analysis, which follows the standard transverse momentum analysis technique of Danielewicz and Odnyc [24], employs a gate,  $0.485 \leq m_{inv} \leq 0.505$  GeV, centered on the invariant mass peak to ensure a relatively pure sample ( $\sim 90 - 92\%$ ) of  $K_s^0$ 's ( $\sim 12060$   $K_s^0$ 's above background). The gate is represented by the hatched area shown in Fig. 1. The orientation of the reaction plane vector  $\mathbf{Q}$  was determined for each event  $i$ , by summing over protons and light nuclei ( $j$ ), with charge  $Z \leq 2$  in events associated with a selected impact-parameter range [25];  $\mathbf{Q}_i = \sum_j w(y_j) \mathbf{p}_j^t / |\mathbf{p}_j^t|$ . Here,  $\mathbf{p}_j^t$  and  $y_j$  represent the transverse momentum vector and rapidity, respectively for baryon  $j$ . The weight  $w(y_j)$  is assigned the value  $\langle p^x \rangle / \langle p^t \rangle$  where  $\langle p^x \rangle$  is the transverse momentum in the reaction plane for baryons.  $\langle p^x \rangle$  is obtained from the first pass of an iterative procedure. The orientation of the impact parameter vector is random. Therefore, the distribution of the determined reaction plane should be uniform (flat). We have established that deviations from this uniformity are the direct result of deficiencies in the acceptance of the TPC and have applied rapidity and multiplicity dependent corrections following Ref. [21]. Such corrections ensure the absence of spurious flow signals which could result from distortions in the reaction plane distribution. The dispersion of the reaction plane,  $\langle \phi_{12} \rangle / 2$  is estimated via the the sub-event method [24] to be  $\sim 37^\circ$  and  $\sim 33^\circ$  for central and mid-central events respectively.

The mean transverse momenta  $\langle p^x \rangle$ , of  $K_s^0$ 's in the reaction plane are shown as a function of the normalized c.m rapidity,  $y_0$  in Fig. 3. Here  $y_0 = y_{Lab} / y_{cm} - 1$ ;  $y_{Lab}$  is the rapidity of the emitted particle in the Lab, and  $y_{cm}$  is the rapidity of the c.m. The  $\langle p^x \rangle$  value shown for each rapidity bin (filled stars) in Fig. 3 includes a small correction for, (a) the effect of the  $\sim 8-10\%$  combinatoric background and (b) inefficiencies associated with the detection of the  $K_s^0$ . The correction for the combinatoric background has been made by evaluating the  $\langle p^x \rangle$  [for each rapidity bin] for the experimental combinatoric background followed by a weighted subtraction of these values from the  $\langle p^x \rangle$  values obtained for the invariant mass selection indicated in Fig. 1. It is important to note here that the magnitude of the flow for the combinatoric background is on average  $\sim 4-5$  times smaller than that for the  $K_s^0$ 's. Thus, the net effect of the background would be an apparent reduction in the flow. The procedure employed to evaluate the flow is as follows. First, for each rapidity selection, we evaluate the  $\langle p^x \rangle$  as a function of  $p^t$  over the range 0 - 0.7 GeV/ $c$ . For this  $p^t$  range the  $\langle p^x \rangle$  shows a linear dependence

[on  $p^t$ ] with a negative slope. Following this evaluation, we determine and correct the  $K_s^0 p^t$  distributions for the same rapidity selection. Estimates for these efficiency corrections have been obtained by tagging and embedding simulated  $K_s^0$ 's [with a flat input  $p^t$  distribution for each  $y$ ] in raw data events in a detailed GEANT simulation of the TPC. Subsequently, a weighted average (obtained by folding the corrected  $p^t$  distribution with the  $p^t$ -dependence of  $\langle p^x \rangle$  for that  $y$  bin) was performed to obtain the  $\langle p^x \rangle$  as a function of rapidity selection. It is noteworthy that this procedure takes account of an  $\sim 10\%$  correction to the flow resulting from the detection efficiency for  $K_s^0$ 's.

The representative  $\langle p^x \rangle$  values shown in Fig. 3 are for  $p^t \leq 700$  MeV/c, and  $b \lesssim 7$  fm. The limited acceptance for  $K_s^0$  detection at negative rapidities results in an apparent cut-off for  $y_0 \leq -0.30$ . The  $\langle p^x \rangle$  values clearly follow an anti-flow pattern. Similarly prominent antiproton patterns have been obtained for more central and less central events. A correction factor of 1.44, has been applied to the data shown in Fig. 3 to account for the reaction plane dispersion [26–28]. A linear fit to these data yields a slope of  $-127 \pm 20$  MeV/c. The dotted and dot-dashed curves shown in Fig. 3 represent flow results obtained from RQMD [18] calculations for  $K_s^0$ 's and protons respectively. The calculations, which have been performed for the same impact parameter and  $p_t$  range as that for the data, include the effects of a mean-field as well as rescattering. However, they do not include the kaon-nucleon potential. Fig. 3 shows calculated trends for protons which are in qualitative agreement with the data [29]. By contrast, the experimental flow pattern observed for  $K_s^0$ 's is clearly at odds with the results obtained from the calculations. This difference is particularly striking for the comparison of both the magnitude and sign of the flow. Here, it is important to stress that unlike pions,  $K_s^0$ 's have a long mean free path in nuclear matter due to their rather small scattering cross section ( $\sigma_{K^0+p} \sim 10$  mb and  $\sigma_{\pi+p} \sim 100$  mb). This being the case, one cannot account for the antiproton flow of  $K^0$ 's via the reabsorption mechanism commonly exploited to explain pion anti-flow [30]. Thus, we attribute the disagreement between data and theory to the absence of an appropriate kaon-nucleon potential in RQMD, and conclude that the experimentally observed flow pattern [for  $K_s^0$ 's] is more consistent with predictions for a strong influence of the repulsive kaon vector potential in the nuclear medium [12,13].

In sum, we have measured the transverse flow of neutral strange  $K_s^0$  mesons in central and mid-central 6AGeV Au+Au collisions. The data show a clear anti-flow signal which is in stark contrast to that observed for protons at the same beam energy. This contrast is more pronounced than for lower energies and a smaller system size [14], possibly because the effects of the repulsive kaon mean field become more significant with the higher baryon densities expected at 6 AGeV. Our sideways flow data, while apparently different from those for the  $^{58}\text{Ni} + ^{58}\text{Ni}$  system

(1.93 AGeV) [14], are not incompatible with the conclusions drawn about the role of the vector potential.

This work was supported in part by the U.S. Department of Energy under grants DE-FG02-87ER40331, DE-FG02-89ER40531, DE-FG02-88ER40408, DE-FG02-87ER40324, and contract DE-AC03-76SF00098; by the US National Science Foundation under Grants PHY-98-04672, PHY-9722653, PHY-96-05207, PHY-9601271, and INT-9225096; by the University of Auckland Research Committee, NZ/USA Cooperative Science Programme CSP 95/33; and by the National Natural Science Foundation of P.R. China under grant 19875012.

- 
- [1] C. M. Ko and G. Q. Li, J. Phys. G22, 1673 (1996)
  - [2] S. A. Bass, et al., J.Phys. G25, R1, (1999)
  - [3] G. E. Brown et al. Nucl. Phys. A567, 937 (1994)
  - [4] G. Q. Li et al., Nucl. Phys. A625, 372 (1997)
  - [5] V. Thorsson et al., Nucl. Phys. A572, 693 (1994)
  - [6] J. W. Harris et al., Annu. Rev. Part. Sci. 46, 71 (1996)
  - [7] D. B. Kaplan et al., Phys. Lett. B175, 57 (1986)
  - [8] G. E. Brown et al., Phys. Rev. C43, 1881, (1991)
  - [9] T. Waas et al., Phys. Lett. B379, 34 (1996)
  - [10] J. Schaffner et al., Phys. Rev. C53, 1416 (1996)
  - [11] M. Lutz, Phys. Lett. B 426, 12 (1998)
  - [12] G.Q. Li, et al., Phys. Rev. Lett. 74, 235 (1995), Bao-An Li et al., Phys. Rev. C60, 3492, (1999)
  - [13] Z. S. Wang, et al., nucl-th/9809043, (1998)
  - [14] J. Ritman et al., Z Phys. A352, 355, (1995)
  - [15] C. David et al., Nuc. Phys. A nucl-th/9805017
  - [16] Y. Shin et al., Phys. Rev. Lett. 81, 1576 (1998)
  - [17] G. Rai et al., IEEE Trans. Nucl. Sci. 37, 56 (1990)
  - [18] H. Sorge Phys. Rev. C52, 3291, (1995)
  - [19] P. Chung et al., (E895 Collaboration) Journal of Phys. G., 25, 255 (1999)
  - [20] G. Bauer et al., NIM A386, 249 (1997)
  - [21] C. Pinkenburg et al. (E895 Collaboration), Phys. Rev. Lett. 83, 1295 (1999)
  - [22] D. Best for the E895 Collaboration, J. Phys. G: Nucl. Part. Phys. 23, 1873, (1997)
  - [23] M. Justice, Nucl. Instrum. Methods Phys. Res. A 400, 463 (1997)
  - [24] P. Danielewicz and G. Odyniec, Phys. Lett. B157,146 (1985)
  - [25] Unique separation of  $\pi^+$ 's and protons was not achieved for all rigidities. Consequently, a small fraction of  $\pi^+$ 's were included in the sample used to determine the reaction plane. The small influence of this pion contamination on the extracted flow value is accounted for via the dispersion correction for the reaction plane.
  - [26] P. Danielewicz et al., Phys. Rev. C 38, 120,(1988).
  - [27] J.-Y. Ollitrault, nucl-ex/9711003 v2.
  - [28] A. M. Poskanzer and S. A. Voloshin, Phys. Rev C58, 1671, (1998)
  - [29] H. Liu et al. (E895 Collaboration)

*Quark Matter '97, Proc. 13th Int. Conf. on Ultra-Relativistic Nucleus-Nucleus Collisions, Tsukuba, Japan, 1997*, ed. P. T. Hatsuda *et al.*, Nucl. Phys. **A638**, 451c (1998), H. Liu *et al.* (E895 Collaboration) Phys. Rev Let. (submitted).

[30] H. Oeschler, IKDA 98/20 Report, (1998).

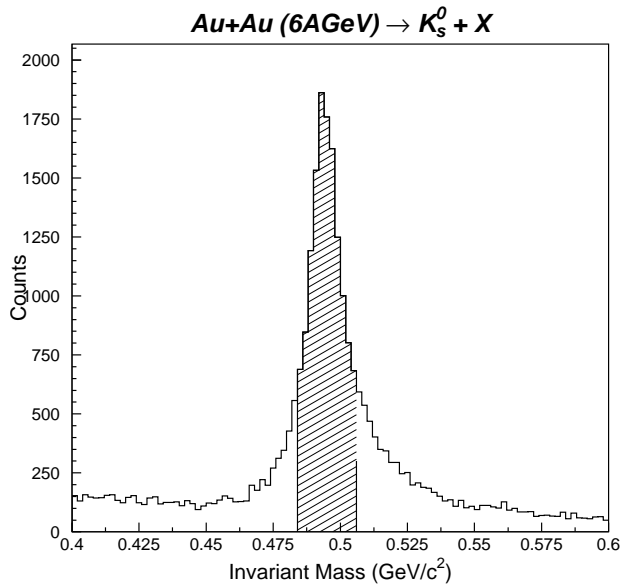


FIG. 1. (a) Invariant mass distribution for  $K_s^0$ . The hatched area indicates accepted  $K_s^0$  particles.

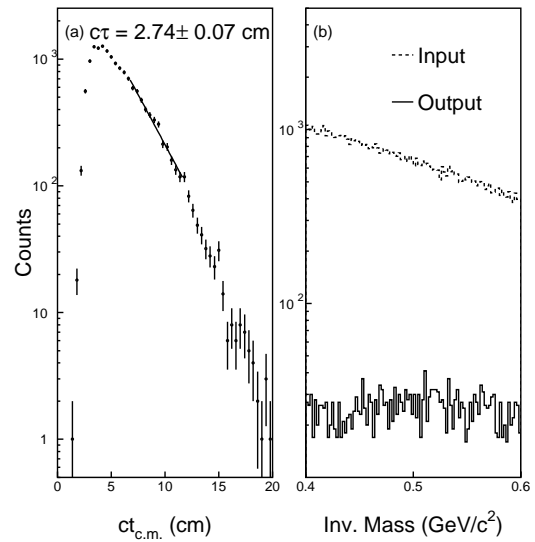


FIG. 2. (a) Decay-length distribution in the rest frame of the  $K_s^0$ . The solid curve is an exponential fit to the data (see text). (b) Invariant mass distributions for combinatoric events processed by the neural network (see text). The input and output distributions are represented by the dotted and solid curve respectively.

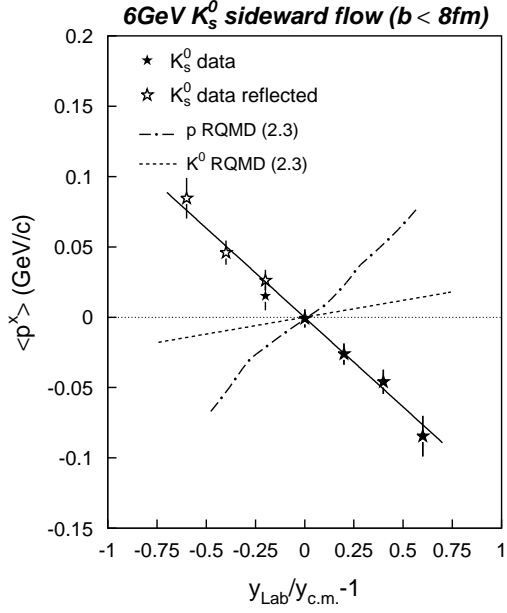


FIG. 3. Experimental  $\langle p^x \rangle$  vs  $y_0$  for  $K_s^0$  mesons (stars).  $\langle p^x \rangle$  values have been corrected for reaction plane dispersion. The solid curve represents a linear fit to the data. Error bars are statistical. The dashed-dot and dotted curves represent results obtained for protons and  $K_s^0$ 's from RQMD v (2.3) (with mean-field). The RQMD results have been obtained for the same impact parameter and  $p^t$  selection as that for the data.